

Analyzing and Improving Stein Variational Gradient Descent for High-dimensional Marginal Inference

Jingwei Zhuo, Chang Liu, Ning Chen, Bo Zhang

Dept. of Comp. Sci. & Tech., State Key Lab of Intell. Tech. & Sys., TNLIS Lib,

Tsinghua University, Beijing, 100084, China

{zjw15@mails., chang-li14@mails, ningchen@, dcszb@}tsinghua.edu.cn

Abstract

Stein variational gradient descent (SVGD) is a nonparametric inference method, which iteratively transports a set of randomly initialized particles to approximate a differentiable target distribution, along the direction that maximally decreases the KL divergence within a vector-valued reproducing kernel Hilbert space (RKHS). Compared to Monte Carlo methods, SVGD is particle-efficient because of the repulsive force induced by kernels. In this paper, we develop the first analysis about the high dimensional performance of SVGD and demonstrate that the repulsive force drops at least polynomially with increasing dimensions, which results in poor marginal approximation. To improve the marginal inference of SVGD, we propose Marginal SVGD (M-SVG), which incorporates structural information described by a Markov random field (MRF) into kernels. M-SVG inherits the particle efficiency of SVGD and can be used as a general purpose marginal inference tool for MRFs. Experimental results on grid based Markov random fields show the effectiveness of our methods.

Introduction

Stein variational gradient descent (SVGD) [13] is a nonparametric inference method for intractable distributions with differentiable densities. To approximate a target distribution, it constructs a set of particles iteratively along optimal gradient direction in a vector valued reproducing kernel Hilbert space (RKHS) for minimizing KL divergence to the target. Theoretical analysis [11] proves that under some mild conditions, SVGD converges to the target distribution asymptotically with infinite particles. SVGD combines advantages of both variational inference (VI) and Markov chain Monte Carlo (MCMC) methods in that it does not confine the approximation within parametric families as commonly done in traditional VI methods, and it converges faster than MCMC due to the deterministic updates that efficiently leverage gradient information. Besides, SVGD is particle-efficient in the sense it generates diverse particles due to the repulsive force induced by kernels. A nice property of SVGD is that when only a single particle is used, it degrades to the gradient descent to get a maximum a posterior (MAP) estimate.

As the only source of diversity, the choice of kernels plays an important role in SVGD. In previous work, kernels are chosen to be based on the Euclidean distance measuring global similarity, with the implicit assumption that particles are diverse in the sense their Euclidean distance is large. However, as discussed in [1] and [16], Euclidean distance and corresponding kernels have poor high dimension performance. Thus, a natural question is, given a finite number of particles, how the performance of SVGD changes as the dimension increases?

In this paper, we show that, due to the deterministic updates and the Euclidean distance based kernels, the repulsive force drops at least polynomially with increasing dimension. leading to less diverse particles for marginals and thus poor marginal approximation with finite particles. In other words, SVGD particles may

approximate the joint distribution well, but the marginal approximation is undesirable. This is different from Monte Carlo methods, where the particles play the same role in approximating the joint distribution and the marginal distribution because of the random nature.

However, marginal approximation is an important problem in machine learning. For example, learning the parameters of Markov random fields (MRFs) requires the marginal distribution as an inner step. And inferring latent variable models also require the marginals. To improve the marginal inference of SVGD, we propose Marginal SVGD (M-SVGD). Compared to SVGD, M-SVGD constructs kernels based on a local similarity measure over the Markov blanket described in MRFs, which solves the decreasing repulsive force problem and generates high quality particles for marginal approximation.

Besides, the computation of M-SVGD is fully local, which makes it suitable as a general purpose marginal inference tool for MRFs. Traditional VI methods for MRFs include mean-field (MF) and belief propagation (BP) algorithms [9], but MF suffers from the strongly independence assumptions and BP requires further approximation in message to handle complex potentials, which restricts its expressive power [18, 8, 10]. Another drawback of BP is that except some special cases where beliefs are tractable (e.g., in the Gaussian BP), numerical integration is required when using beliefs in subsequent tasks like evaluating the expectation over some test functions. On the other hands, sampling methods like Gibbs sampling get rid of this as the expectation can be computed directly over samples. However, Gibbs sampling can only be used in some special cases where the conditional distribution can be sampled efficiently [14]. Some other methods do exist [2], but they introduce extra restrictions to the potentials, e.g., continuous constrained MRFs (CCMRFs) with linear constraints and hinge loss like potentials. Compared to these methods, M-SVGD is more appealing, because it does not require either tractable conditional distribution or restrictions over potentials.

In summary, we make two main contributions:

1. We analyze the impact of dimension on the performance of SVGD, and show that SVGD suffers from poor marginal approximation because of the decreasing repulsive force. We also discuss the importance of kernel bandwidth on the performance of SVGD, and point out that the median heuristic [17] is somehow the best bandwidth choice.
2. We propose Marginal SVGD (M-SVGD) as a marginal inference counterpart of SVGD to provide high quality marginal approximation. M-SVGD inherits the advantages of SVGD compared to traditional variational inference and MCMC methods and can be applied to any marginal inference problem for MRFs with differentiable potentials.

Preliminaries

Given an intractable distribution $p(x)$ where $x = (x_1, \dots, x_D) \in \mathbb{R}^D$, variational inference tries to find a tractable distribution $q(x)$ to approximate $p(x)$ by minimizing $KL(q||p)$. Instead of assigning a parametric assumption over $q(x)$, Stein variational gradient descent (SVGD) [13] constructs $q(x)$ from some initial $q_0(x)$ via a sequence of density transformation induced by $T(x) = x + \epsilon\phi(x)$, where ϵ is the step size and $\phi : \mathbb{R}^D \rightarrow \mathbb{R}^D$ denotes the transport direction. To be tractable and flexible, ϕ is restricted to a vector valued reproducing kernel Hilbert space (RKHS) $\mathcal{H}^D = \mathcal{H}_0 \times \dots \times \mathcal{H}_0$, where \mathcal{H}_0 is a scalar valued RKHS associated with positive definite kernel $k(\cdot, \cdot) : \mathbb{R}^D \times \mathbb{R}^D \rightarrow \mathbb{R}$. In previous work, kernels are chosen to measure global similarity, i.e.,

$$k(x, y) = k(x - y) = f\left(\frac{\|x - y\|_2^2}{2\gamma^2}\right), \quad (1)$$

where γ^2 is the bandwidth and is chosen according to the median heuristic [17], i.e., $\gamma^2 = \text{med}^2$, where med is the median of the pairwise distance $\|x - y\|_2^2, \forall x, y \in q$. f is a smooth function with bounded derivative

and satisfies $\lim_{z \rightarrow \infty} f(z) = 0$, $\lim_{z \rightarrow 0} f(z) = 1$. Examples include the RBF kernel $f(z) = \exp(-z)$ [13] and the IMQ kernel $f(z) = 1/\sqrt{1+z}$ [6].

Now, let $q_{[\epsilon\phi]}$ denote the density of $T(x) = x + \epsilon\phi(x)$ when $x \sim q$, if ϵ is small enough so that T is an invertible mapping, the derivative of the steepest direction of KL divergence satisfies

$$\min_{\phi \in \mathcal{H}^D} \nabla_{\epsilon} KL(q_{[\epsilon\phi]} || p)|_{\epsilon=0} = - \max_{\phi \in \mathcal{H}^D} \mathbb{E}_{x \sim q} [\mathcal{A}_p \phi(x)], \quad (2)$$

where \mathcal{A}_p is the Stein operator and

$$\mathcal{A}_p \phi(x) = \phi(x)^T \nabla_x \log p(x) + \text{trace}(\nabla_x \phi(x)).$$

As shown in [12] and [3], the right hand side of Eq. 2 has a closed-form solution, which is the so-called Stein variational gradient

$$\phi^*(x) = \mathbb{E}_{y \sim q} [k(x, y) \nabla_y \log p(y) + \nabla_y k(x, y)]. \quad (3)$$

As a result, $q_{[\epsilon\phi^*]}$ decreases the KL divergence along the steepest direction from q . By doing the transformation $x \leftarrow x + \epsilon\phi^*(x)$ iteratively until $\phi^*(x) = 0$, the KL divergence finally converges to a local optimum and the final q will be the variational approximation for p .

In practice, $q(x)$ is approximated by $\hat{q}_M = \frac{1}{M} \sum_{i=1}^M \delta_{x^{(i)}}(x)$ with a set of particles $\{x^{(i)}\}_{i=1}^M$, which are initialized randomly according to some prior $q_0(x)$. These particles are updated via $x^{(i)} \leftarrow x^{(i)} + \epsilon\hat{\phi}^*(x^{(i)})$ with the empirical Stein variational gradient

$$\hat{\phi}^*(x) = \mathbb{E}_{y \in \hat{q}_M} [k(x, y) \nabla_y \log p(y) + \nabla_y k(x, y)]. \quad (4)$$

$\hat{\phi}^*(x)$ contains two parts: the kernel smoothed gradient $\mathbb{E}_{y \sim \hat{q}_M} [k(x, y) \nabla_y \log p(y)]$ which corresponds to the steepest direction for the log probability, and the repulsive force $\mathbb{E}_{y \sim \hat{q}_M} [\nabla_y k(x, y)]$ which enforces the diversity (induced by kernels) among particles. When $M = 1$, SVGD degrades to the gradient method for maximum a posteriori (MAP).

Our Contributions

Our contributions are twofold: first, we analyze the high dimensional performance of SVGD, discuss the importance of bandwidth choice and give mathematical reasoning on a special case to support our claim; second, we propose Marginal SVGD as a counterpart of SVGD to generate high quality particles for marginal inference of Markov random fields (MRFs).

SVGD Fails in Marginal Inference in High Dimensions

We first give an intuition about why SVGD with finite particles fails in marginal inference in high dimension, and we use Gaussian distribution as a demonstrative example.

In kernel-based methods, choosing a proper bandwidth is very important. Too large or too small bandwidth will overestimate or underestimate the similarity and both cases deteriorate the power of kernels in measuring similarity. Given the kernels measuring global similarity, e.g., the RBF kernel¹ $k(x, y) = \exp\left(-\frac{\|x-y\|_2^2}{2\gamma^2}\right)$, a

¹The IMQ kernel $k(x, y) = 1/\sqrt{1 + \frac{1}{2\gamma^2}\|x-y\|_2^2}$ also holds the same property, which can be verified following the same derivation.

proper bandwidth γ^2 should be on the same order of $\|x - y\|_2^2$, e.g., the median heuristic. However, recall that the d th dimension of empirical Stein variational gradient is

$$\begin{aligned}\hat{\phi}_d^*(x) = & \mathbb{E}_{y \sim \hat{q}_M} \left[\exp \left(-\frac{\|x - y\|_2^2}{2\gamma^2} \right) \nabla_{y_d} \log p(y) \right. \\ & \left. + \exp \left(-\frac{\|x - y\|_2^2}{2\gamma^2} \right) \frac{y_d - x_d}{\gamma^2} \right],\end{aligned}\quad (5)$$

where γ^2 appears as a denominator both for $\|x - y\|_2^2$ (global similarity) and $y_d - x_d$ (local similarity), which are not on the same order and the latter is roughly D times smaller than the former. As a result, choosing a proper γ^2 in SVGD is much harder than other kernel-based methods, e.g., kernel density estimation, in which γ^2 only appears as a denominator for $\|x - y\|_2^2$.

In fact, a proper γ^2 does not exist in general. To see this, note that $\mathbb{E}_{x, y \sim \hat{q}_M} [\|x - y\|_2^2] = 2 \sum_{d=1}^D \text{Var}_{\hat{q}_M}(x_d)$. Given finite particles, and further assuming that the marginal variance is uniformly bounded, i.e., $\exists C_1, C_2 > 0$, such that $C_1 \leq \text{Var}_{\hat{q}_M}(x_d) \leq C_2, \forall d \in \{1, \dots, D\}$, we have $\mathbb{E}_{x, y \sim \hat{q}_M} [\|x - y\|_2^2] \propto D$. As discussed in [16], med^2 is on the same order of $\mathbb{E}_{x, y \sim \hat{q}_M} [\|x - y\|_2^2]$ and thus the median heuristic can be regarded as the case when $\gamma^2 \propto D$. Without loss of generality, suppose $\gamma^2 \propto D^{1+\epsilon}$ with some $\epsilon \geq -1$, we have $\frac{\|x - y\|_2^2}{2\gamma^2} \propto D^{-\epsilon}$ and $\frac{x_d - y_d}{\gamma^2} \propto D^{-1-\epsilon}$, respectively.

As a result, we can discuss three different choices for γ^2 and its influence in the behaviour of $\hat{\phi}^*(x)$ as $D \rightarrow \infty$:

- **Underestimated bandwidth** ($-1 \leq \epsilon < 0$): as $D \rightarrow \infty$, $\exp \left(-\frac{\|x - y\|_2^2}{2\gamma^2} \right) \rightarrow 0$ for $x \neq y$ while $\frac{x_d - y_d}{\gamma^2} \rightarrow 0$ ($-1 < \epsilon < 0$) or be of order 1 ($\epsilon = -1$). In this case, the repulsive force decreases to zero and $\phi^*(x) \approx \nabla_{x_d} \log p(x)$. As a result, SVGD degrades to M independent gradient descent with random initialization and the particles $\{x^{(i)}\}_{i=1}^M$ will converge to local modes.
- **Overestimated bandwidth** ($\epsilon > 0$): as $D \rightarrow \infty$, $\exp \left(-\frac{\|x - y\|_2^2}{2\gamma^2} \right) \rightarrow 1$ while $\frac{x_d - y_d}{\gamma^2} \rightarrow 0$. In this case, the repulsive force also decreases to zero and $\phi^*(x) \approx \frac{1}{M} \sum_{i=1}^M \nabla_{x_d} \log p(x^{(i)})$. In other words, all the particles share the same Stein variational gradient.
- **Median heuristic** ($\epsilon = 0$): as $D \rightarrow \infty$, $\exp \left(-\frac{\|x - y\|_2^2}{2\gamma^2} \right)$ is of order 1 while $\frac{x_d - y_d}{\gamma^2} \rightarrow 0$. In this case, the repulsive force still decreases to zero and $\phi^*(x) \approx \frac{1}{M} \sum_{i=1}^M \exp \left(-\frac{\|x - x^{(i)}\|_2^2}{2\gamma^2} \right) \nabla_{x_d} \log p(x^{(i)})$.

As is discussed, for high dimensional case as $D \rightarrow \infty$, because of the imbalance of order of magnitude between $\|x - y\|_2^2$ and $x_d - y_d$, the repulsive force $\mathbb{E}_{y \sim \hat{q}_M} \left[\exp \left(-\frac{\|x - y\|_2^2}{2\gamma^2} \right) \frac{y_d - x_d}{\gamma^2} \right]$ will drop to zero no matter which γ^2 is used. As a result, the performance of SVGD will largely depend on the kernel smoothed gradient $\mathbb{E}_{y \sim \hat{q}_M} \left[\exp \left(-\frac{\|x - y\|_2^2}{2\gamma^2} \right) \nabla_y \log p(y) \right]$.

Given this intuition, a natural question is, how fast the repulsive force decreases with increasing dimension? If we regard $\exp \left(-\frac{\|x - y\|_2^2}{2\gamma^2} \right) \frac{|y_d - x_d|}{\gamma^2}$ as a function of γ^2 , by using derivative we can find that when $\gamma^2 = \|x - y\|_2^2 / |x_d - y_d|$, it attains its maximum, which is $\exp(-|x_d - y_d|) \frac{(x_d - y_d)^2}{\|x - y\|_2^2} \propto 1/D$ and decreases to zero by a factor of $1/D$. In the next section, we will verify this on a special case when $q(x)$ is a Gaussian distribution² by using mathematical reasoning.

²The variational distribution $q(x)$ to be a Gaussian distribution is a quite strong assumption and this may not be the case in practice, as particles $\{x^{(i)}\}_{i=1}^M$ may be from any distribution. However, this will give us some mathematical insights about SVGD, and experiments in the next section verify these insights.

A Demonstrating Example of Gaussian

Note that the empirical gradient $\hat{\phi}^*(x)$ over a set of particles $\{x^{(i)}\}_{i=1}^M$ is an unbiased estimate of $\phi^*(x)$. Thus, we can analyse $\phi^*(x)$ to give a strong intuition about the performance of $\hat{\phi}^*(x)$. First, we'd like to introduce the following lemma.

Lemma 1. Suppose $p(x) = \mathcal{N}(x|\mu_p, \Sigma_p)$ and a RBF kernel $k(x, y) = \exp(-\frac{\|x-y\|_2^2}{2\gamma^2})$ is used, when $q(x) = \mathcal{N}(x|\mu_q, \Sigma_q)$, the Stein variational gradient satisfies $\phi^*(x) = g(x)(U_1 + U_2(x))$, where

$$g(x) = \frac{\sqrt{\det \Sigma_q^{-1}}}{\sqrt{\det(\Sigma_q^{-1} + \gamma^{-2}I)}} \exp\left(-\frac{1}{2}d(x, \mu_q)\right)$$

with $d(x, \mu_q) = (x - \mu_q)^T(\Sigma_q + \gamma^2 I)^{-1}(x - \mu_q)$ and

$$U_1 = \Sigma_p^{-1}(\mu_p - \mu_q),$$

$$U_2(x) = \frac{1}{\gamma^2}(I - (\Sigma_p^{-1} + \gamma^{-2}I)(\Sigma_q^{-1} + \gamma^{-2}I)^{-1})(x - \mu_q).$$

Recall that SVGD is converged when $\phi^*(x) = 0, \forall x$, which corresponds to $\mu_q = \mu_p$ and $\Sigma_p = \Sigma_q$. An important observation from Lemma 1 is that we can decompose $\phi^*(x)$ into two terms: $g(x)U_1$ is the mode-matching term which equals zero as long as $\mu_q = \mu_p$, and $g(x)U_2(x)$ is the variance-matching term which equals zero as long as $\Sigma_q = \Sigma_p$. We'd like to verify the relationship between $g(x)U_2(x)$ and the dimensionality D . For simplicity, we only discuss the spherical Gaussian case, although the result also holds for the full covariance Gaussian³.

Corollary 1. Suppose $\Sigma_q = \sigma_q^2 I$,

$$\|g(x)U_2(x)\|_2 \leq \frac{C}{\gamma^2(1 + \sigma_q^2/\gamma^2)^{D/2}}\|x - \mu_q\|_2,$$

and

$$\|g(x)U_2(x)\|_\infty \leq \frac{C\sqrt{D}}{\gamma^2(1 + \sigma_q^2/\gamma^2)^{D/2}}\|x - \mu_q\|_\infty,$$

holds for any $x \in \mathbb{R}^D$.

Corollary 1 provides a bound for $g(x)U_2(x)$ with $x - \mu_q$ which depends on D and γ^2 . We will show that this bound decreases to zero as D increases for all the bandwidth choices.

Observation 1. Suppose $\gamma^2 = \sigma_q^2 D^{1+\epsilon}$ ($\epsilon \geq -1$), we have

$$\|g(x)U_2(x)\|_2 \leq \frac{C}{\sigma_q^2 D^{1+\epsilon}(1 + D^{-1-\epsilon})^{D/2}}\|x - \mu_q\|_2,$$

and

$$\|g(x)U_2(x)\|_\infty \leq \frac{C}{\sigma_q^2 D^{1/2+\epsilon}(1 + D^{-1-\epsilon})^{D/2}}\|x - \mu_q\|_\infty.$$

- **Underestimated bandwidth** ($-1 \leq \epsilon < 0$): the upper bounds on $\|g(x)U_2(x)\|_2$ and $\|g(x)U_2(x)\|_\infty$ decrease to zero exponentially as $D^{-1-\epsilon}/\exp(D^{-\epsilon}/2)\|x - \mu_q\|_2$ and as $D^{-1/2-\epsilon}/\exp(D^{-\epsilon}/2)\|x - \mu_q\|_\infty$ respectively.

³Details can be found in the supplementary materials.

- **Overestimated bandwidth** ($\epsilon > 0$), the upper bounds on $\|g(x)U_2(x)\|_2$ and $\|g(x)U_2(x)\|_\infty$ decrease to zero polynomially as $1/D^{1+\epsilon}\|x - \mu_q\|_2$ and as $1/D^{1/2+\epsilon}\|x - \mu_q\|_\infty$ respectively.
- **Median heuristic** ($\epsilon = 0$), the upper bounds on $\|g(x)U_2(x)\|_2$ and $\|g(x)U_2(x)\|_\infty$ decrease to zero polynomially as $1/D\|x - \mu_q\|_2$ and as $1/D^{1/2}\|x - \mu_q\|_\infty$ respectively.

As is shown in Observation 1, the median heuristic is the best possible bandwidth in the sense that it corresponds to the slowest decrease of $g(x)U_2(x)$ with increasing dimension. However, in all cases, $\|g(x)U_2(x)\|_2/\|x - \mu_q\|_2 \rightarrow 0$ and $\|g(x)U_2(x)\|_\infty/\|x - \mu_q\|_\infty \rightarrow 0$ as $D \rightarrow \infty$. In other words, assuming x is bounded, the variance-matching term $g(x)U_2(x)$ converges to 0 uniformly as D increases⁴, which coincides with the discussion in the last section.

Another interesting observation is that when $\mu_p = \mu_q$ and thus $U_1 = 0$, $\phi^*(x) = g(x)U_2(x)$. In other words, when q matches p in the mean, the Stein variational gradient $\phi^*(x)$ will fully depend on the variance-matching term $g(x)U_2(x)$, whose magnitude decreases at least polynomially with increasing dimensions. For any $x, y \in \mathbb{R}^D$ satisfying $x \neq y$, the difference between their Stein variational gradient $\|\phi^*(x) - \phi^*(y)\| \leq \|\phi^*(x)\| + \|\phi^*(y)\|$ also decreases. As a result, SVGD loses its power in the sense that any $x \in \mathbb{R}^D$ has a similar $\phi^*(x)$, which results in slow convergence in high dimensions, as shown in Figure 2.

Marginal SVGD: Generating High Quality Particles For Marginal Approximation

As discussed in the last section, the poor marginal approximation phenomenon comes from Eq. 5, in which a global similarity measure shared by every dimension leads to a mismatch of bandwidth, and this mismatch leads to the vanishing repulsive force with increasing dimension.

To overcome this mismatch, an intuitive idea is to use a local similarity measure for each dimension, and thus the bandwidth can be chosen properly. More specifically, instead of restricting ϕ in an isotropic vector valued RKHS $\mathcal{H}^D = \mathcal{H}_0 \times \dots \times \mathcal{H}_0$ where \mathcal{H}_0 shares the kernel k measuring global similarity in \mathbb{R}^D , we'd like to restrict it in an anisotropic vector valued RKHS $\mathcal{H}^D = \mathcal{H}_1 \times \dots \times \mathcal{H}_D$ where \mathcal{H}_d is associated with the kernel k_d measuring local similarity in the d th dimension.

However, such a local kernel is hard to define in general. On the one hand, we hope the kernel depends on a low dimensional space so that the mismatch of bandwidth will be alleviated. On the other hand, we require the transform ϕ_d to be flexible enough so the rich representation ability of SVGD will not lose. Naively defining k_d only on the d th dimension (i.e., $k_d(x_d, y_d) : \mathbb{R} \times \mathbb{R} \rightarrow \mathbb{R}$) is not a good choice, as it corresponds to the transformation $x_d \leftarrow x_d + \epsilon\phi_d(x_d)$ which equals the mean field approximation and loses all the flexibility of SVGD in approximating complex distributions. So, we need a kernel defined on minimum number of dimensions which maximally maintains the possible dependency properties. This structural information about dependencies is described by Markov random fields (MRFs)⁵.

By using undirected graphs, MRFs describe the dependencies among random variables. Let $G = (V, E)$ be an undirected graph in which V denotes the set of nodes (we set $|V| = D$) and E the set of edges. Each node $s \in V$ has a corresponding random variables $X_s \in \mathbb{R}$ and we define the potentials for each node and each edge as $\psi_d(x_d)$ for node d and $\psi_{dt}(x_d, x_t)$ for edge (d, t) . By doing so, the MRF defines a class of distributions for $X = (X_1, \dots, X_D)$ with the density satisfying

$$p(x) = \frac{1}{Z} \prod_{d \in V} \psi_d(x_d) \prod_{(d,t) \in E} \psi_{dt}(x_d, x_t), \quad (6)$$

⁴In practice, the condition that x is bounded is satisfied since only finite particles are used.

⁵We discuss pairwise MRFs in this paper, as by selectively introducing auxiliary variables, any MRF can be converted into an equivalent pairwise form[19].

where the partition function is

$$Z = \int_{\mathcal{X}} \prod_{d \in V} \psi_d(x_d) \prod_{(d,t) \in E} \psi_{dt}(x_d, x_t) dx. \quad (7)$$

A nice property of MRFs defined over G is the local Markov property, i.e., $p(x_d|x_{-d}) = p(x_d|x_{\Gamma_d})$, where $-d$ denotes all nodes in V other than d and Γ_d denotes the Markov blanket for node $d \in V$ (i.e., $\Gamma_d = \{t | (d, t) \in E, t \in V\}$). In other words, the Markov blanket contains the minimum set of nodes with all the information needed to evaluate x_d . Thus, for distributions over MRFs, we can define k_d on x_d and its Markov blanket, i.e., $k_d(x_{d,\Gamma_d}, y_{d,\Gamma_d}) : \mathbb{R}^{1+|\Gamma_d|} \times \mathbb{R}^{1+|\Gamma_d|} \rightarrow \mathbb{R}$. As a result, the d th dimension of the empirical Stein variational gradient $\hat{x}_d^*(x)$ becomes

$$\begin{aligned} \hat{\phi}_d^*(x_{d,\Gamma_d}) &= \frac{1}{M} \sum_{j=1}^M k_d(x_{d,\Gamma_d}^{(j)}, x_{d,\Gamma_d}) \nabla_{x_d^{(j)}} \log p(x_d^{(j)} | x_{\Gamma_d}^{(j)}) \\ &\quad + \nabla_{x_d^{(j)}} k_d(x_{d,\Gamma_d}^{(j)}, x_{d,\Gamma_d}). \end{aligned} \quad (8)$$

By updating particles using the Markov blanket based Stein variational gradient defined in Eq. 8, we get a variant of SVGD and we call it Marginal SVGD (M-SVGD) since our purpose is to improve marginal inference. A nice property of M-SVGD is that the computation in Eq. 8 only requires local values, which is particularly suitable for inferring MRFs.

We can define the local kernel as $k_d(x_{d,\Gamma_d}, y_{d,\Gamma_d}) = f(\frac{\|x_{d,\Gamma_d} - y_{d,\Gamma_d}\|_2^2}{2\gamma_d^2})$ where f is the RBF or IMQ kernel, with the implicit assumption that all nodes in the Markov blanket contributes equally to the similarity measure for the d th dimension. However, this definition does not utilize all the structural information in MRFs: it ignores edges between x_d and its Markov blanket. To incorporate this information, we can define the local kernel as $k_d(x_{d,\Gamma_d}, y_{d,\Gamma_d}) = f(\frac{\|x_d - y_d\|_2^2}{2\gamma_d^2}) + \sum_{t \in \Gamma_d} f(\frac{\|x_{d,t} - y_{d,t}\|_2^2}{2\gamma_{dt}^2})$, which is the summation of multiple kernels measuring similarity for x_d itself and edges between x_d and its Markov blanket. We call the former which uses a single kernel as M-SVGD-s and the latter which uses multiple kernels as M-SVGD-m.

Experiments

In this section, we empirically verify our analysis and evaluate the performance of our method on MRFs. In experiments, SVGD and M-SVGD are implemented based on the code of [13] while grid based MRFs are implemented based on the code of [10]. The median heuristic is used to choose a proper bandwidth in all experiments.

Poor Marginal Approximation of SVGD

Our first experiment is designed to verify our analysis for SVGD with finite particles: (1) the marginal approximation of SVGD becomes worse as dimension increases, no matter which bandwidth is chosen; (2) among all the bandwidth choices, the median heuristic is almost the best one in the sense that it balances the convergence speed and marginal particle diversity.

In this experiment, we set the target to be $p(x) = \mathcal{N}(0, I_D)$ as a D dimensional isotropic Gaussian distribution, and use $M = 100$ particles initialized as i.i.d examples from $q_0(x) = \mathcal{N}(x|0, 25I_D)$. We use the RBF kernel $k(x, y) = \exp(\frac{-\|x-y\|_2^2}{\gamma^2})$, in which the bandwidth $\gamma^2 = D^{\alpha-1} \cdot \text{med}^2$ with $\alpha = 1$ the median heuristic, $\alpha > 1$ the overestimated bandwidth and $\alpha < 1$ the underestimated bandwidth. We evaluate the quality of particles in marginal approximation by using the average marginal variance $\frac{1}{D} \sum_{d=1}^D \text{Var}_{\hat{q}_M}(x_d)$,

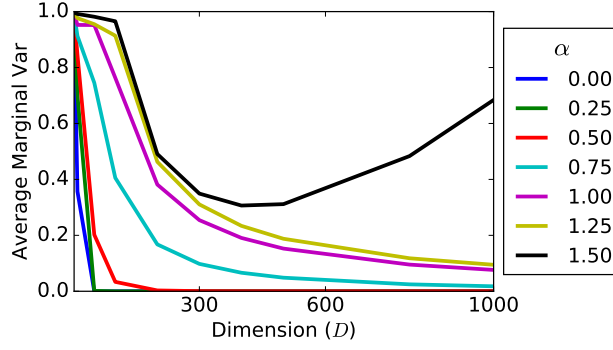


Figure 1: The average marginal variance of particles generated by SVGD with different bandwidth versus dimension.

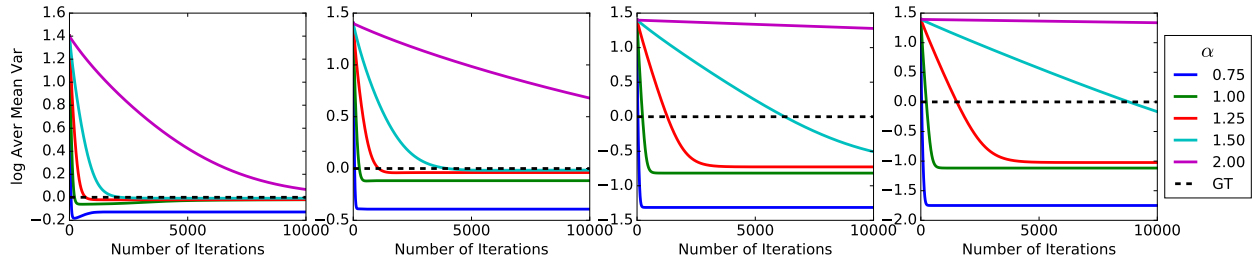


Figure 2: The convergence performance of SVGD with different bandwidth is evaluated for different dimension $D = 50, 100, 500, 1000$ arrange from left to right. “GT” denotes the ground truth, which equals one.

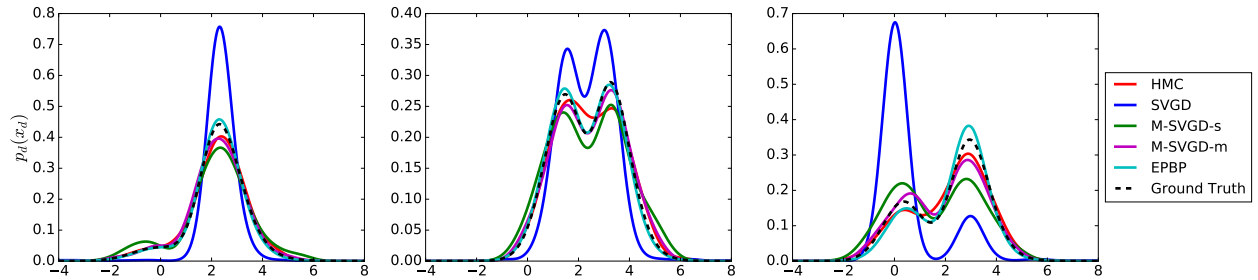


Figure 3: A qualitative comparison of marginal approximation with 100 particles for marginal distributions of three randomly selected nodes. Density curves of SVGD, M-SVGD and HMC are estimated by kernel density estimator with RBF kernels. For EPBP, the curve is drawn by normalizing its beliefs over the fixed interval $[-5, 10]$ with bin size 0.01.

which measures the extent to which the particles are diverse to each other in marginals. The average marginal variance of $p(x)$ is 1. For all experiments, we use Adagrad [5] for step size and execute 10000 iterations to get final particles.

Figure 1 demonstrates the relationship among marginal particle diversity, bandwidth choices and dimensions. An interesting observation is that there exists an inflection point around $D = 400$ in the curve of overestimated bandwidth ($\alpha = 1.5$). The reason is that larger bandwidth leads to smaller $\phi^*(x)$ and thus slower convergence, and this phenomenon deteriorates as dimension increases. Thus, for the bandwidth $\alpha = 1, 5$ and $D > 400$, SVGD cannot converge with 10000 iterations. Excluding this unconverged case, we can find out that as dimension increases, the marginal approximation deteriorates no matter which bandwidth is chosen.

Figure 2 demonstrates the convergence performance of SVGD with different bandwidth. To highlight the difference, we use the log scale in Y axis. As is shown, bandwidth plays an important role in the convergence of SVGD: smaller bandwidth leads to faster convergence. And the gap between different bandwidth becomes larger as dimension increases. Another observation is, when converged, larger bandwidth corresponds to higher marginal variance, which implies more diverse particles and better marginal approximation. Among these bandwidth choices, the median heuristic ($\alpha = 1$) is somehow the best one for two reasons: (1) It converges almost as fast as the underestimated bandwidth ($\alpha < 1$); (2) It achieves almost the best marginal variance. Though overestimated bandwidth ($\alpha > 1$) achieves slightly better performance than the median heuristic when converged, the gap is not as large as that between the median heuristic and underestimated bandwidth. For example, in the rightmost figure, the gap of the average marginal variance between $\alpha = 1.25$ and $\alpha = 1$ is much smaller than that between $\alpha = 0.75$ and $\alpha = 1$.

Grid Based Markov Random Fields

Our second experiment is designed to demonstrate the power of M-SVGD in marginal inference. We follow the settings of [10] and focus on a two-dimensional grid based MRFs with the random variable in each node taking values on \mathbb{R} . The node and edge potentials are chosen such that the marginals are multimodal, non-Gaussian and skewed:

$$\begin{cases} \psi_d(x_d) = \alpha_1 \mathcal{N}(x_d - y_d | -2, 1) + \alpha_2 \mathcal{G}(x_d - y_d | 2, 1.3) \\ \psi_{dt}(x_d, x_t) = \mathcal{L}(x_d - x_t | 0, 2) \end{cases}, \quad (9)$$

where y_d denotes the observed value at node d and is initialized randomly as $y_d \sim \alpha_1 \mathcal{N}(y_d - 2 | -2, 1) + \alpha_2 \mathcal{G}(y_d - 2 | 2, 1.3)$, and $\mathcal{N}(x | \mu, \sigma^2) \propto \exp(-(x - \mu)^2 / (2\sigma^2))$, $\mathcal{G}(x | \mu, \beta) \propto \exp(-(x - \mu)/\beta + \exp(-(x - \mu)/\beta))$ and $\mathcal{L}(x | \mu, \beta) \propto \exp(-|x - \mu|/\beta)$ denote the density of Gaussian distribution, Gumbel distribution and Laplace distribution, respectively. Parameters α_1 and α_2 are set to 0.6 and 0.4. We consider a 10×10 grid in our experiment.

For ground truth of the marginal distribution on each node, we note that it is highly intractable: not even an unnormalized density can be accessed. So we recover the ground truth by marginalizing samples from the joint distribution drawn by No-U-turn sampler (NUTS) [7], a Hamiltonian Monte Carlo (HMC) [4, 15] variant with adaptive path length. We run 100 chains in parallel with 40,000 samples for each chain after 10,000 burned-in, i.e. 4 million samples in total.

We compare our M-SVGD with SVGD, HMC and Expectation Particle Belief Propagation (EPBP) [10]. Although widely used in MRFs, Gibbs sampling does not suit this task since the conditional distribution $p(x_d | x_{\Gamma_d})$ cannot be sampled directly. For HMC, we use uniformly randomly chosen particles from the ground truth samples. This builds a strong baseline. EPBP is a particle-based belief propagation method which achieves the state-of-the-art results for grid based MRFs. Unlike HMC, whose particles are just samples from the target distribution, particles in EPBP are sampled from a Gaussian approximation of beliefs and are used to approximate the message. All experimental results are averaged over 10 runs.

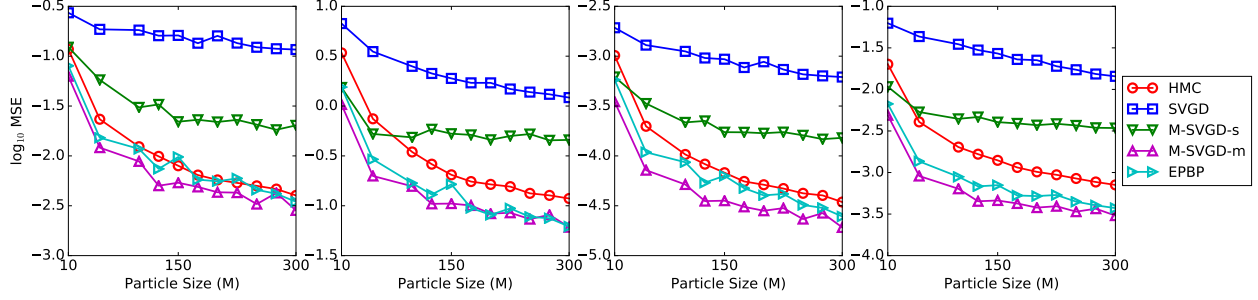


Figure 4: A quantitative comparison of marginal approximation with varying number of particles. Performance is measured by the MSE of the estimation of expectation under marginal distribution for functions x , x^2 , $1/(1 + \exp(\omega x + b))$ and $\cos(\omega x + b)$, arranged from left to right. $\omega, b \in \mathbb{R}^{100}$ with $\omega_d \sim \mathcal{N}(0, 1)$ and $b_d \in \text{Uniform}[0, 2\pi]$, $\forall d \in \{1, \dots, 100\}$. Results are averaged over 10 random draws of ω and b .

Figure 3 provides a qualitative comparison of these methods by visualizing the approximated marginals on each node. As is shown, SVGD approximates the marginals undesirably in all cases. For both unimodal and bimodal cases, SVGD exhibits a sharp, peaked behavior, implying the converging trend of SVGD particles. Another interesting phenomenon appears in the rightmost figure where SVGD skews towards the smaller mode. One possible reason is that the smaller marginal mode corresponds to a larger mode in the joint distribution, into which SVGD particles tends to collapse. Other methods perform similarly in the marginal approximation. Compared to HMC and EPBP, M-SVGD usually underestimates the density around modes, which implies M-SVGD particles are more spread than other methods. Besides, M-SVGD-m has a better approximation than M-SVGD-s, reflecting the benefit of M-SVGD-m to utilize more structural information in local kernels.

Figure 4 provides a quantitative comparison in mean squared error (MSE) of expectation estimation with different particle sizes M . For EPBP, we refer M to the number of node particles when approximating messages. The true expectation is estimated by the 4 million NUTS samples. As is shown, M-SVGD-m performs much better than SVGD and M-SVGD-s, which coincides with the discussion in the qualitative comparison. Compared to HMC and EPBP, M-SVGD-m achieves similar or even better MSE, which demonstrates the particle efficiency of our method. This phenomenon has also been observed in SVGD on 1D Gaussian mixture [13], and the possible reason may be that M-SVGD-m generates more spread particles due to the repulsive force, and hence has the chance to approximate the distribution more smoothly.

Conclusions

In this paper, we analyze the high dimensional performance of Stein variational gradient descent (SVGD), and demonstrate that the repulsive force drops at least polynomially as dimension increases, which leads to poor marginal approximation in high dimensions. We also discuss the importance of bandwidth and indicates that the median heuristic corresponds to the best bandwidth in the sense it achieves a balance between diversity encouragement and convergence performance. We propose marginal SVGD (M-SVGD) to improve marginal inference of SVGD. Experiments on grid based Markov random fields show the effectiveness of M-SVGD.

References

- [1] Charu C Aggarwal, Alexander Hinneburg, and Daniel A Keim. On the surprising behavior of distance metrics in high dimensional spaces. In *ICDT*, volume 1, pages 420–434. Springer, 2001.

- [2] Matthias Broecheler and Lise Getoor. Computing marginal distributions over continuous markov networks for statistical relational learning. In *Advances in Neural Information Processing Systems*, pages 316–324, 2010.
- [3] Kacper Chwialkowski, Heiko Strathmann, and Arthur Gretton. A kernel test of goodness of fit. In *International Conference on Machine Learning*, pages 2606–2615, 2016.
- [4] Simon Duane, Anthony D Kennedy, Brian J Pendleton, and Duncan Roweth. Hybrid monte carlo. *Physics letters B*, 195(2):216–222, 1987.
- [5] John Duchi, Elad Hazan, and Yoram Singer. Adaptive subgradient methods for online learning and stochastic optimization. *Journal of Machine Learning Research*, 12(Jul):2121–2159, 2011.
- [6] Jackson Gorham and Lester Mackey. Measuring sample quality with kernels. *arXiv preprint arXiv:1703.01717*, 2017.
- [7] Matthew D Hoffman and Andrew Gelman. The no-u-turn sampler: adaptively setting path lengths in hamiltonian monte carlo. *Journal of Machine Learning Research*, 15(1):1593–1623, 2014.
- [8] Alexander T Ihler and David A Mcallester. Particle belief propagation. In *International Conference on Artificial Intelligence and Statistics*, pages 256–263, 2009.
- [9] Daphne Koller and Nir Friedman. *Probabilistic graphical models: principles and techniques*. MIT press, 2009.
- [10] Thibaut Lienart, Yee Whye Teh, and Arnaud Doucet. Expectation particle belief propagation. In *Advances in Neural Information Processing Systems*, pages 3609–3617, 2015.
- [11] Qiang Liu. Stein variational gradient descent as gradient flow. *arXiv preprint arXiv:1704.07520*, 2017.
- [12] Qiang Liu, Jason Lee, and Michael Jordan. A kernelized stein discrepancy for goodness-of-fit tests. In *International Conference on Machine Learning*, pages 276–284, 2016.
- [13] Qiang Liu and Dilin Wang. Stein variational gradient descent: A general purpose bayesian inference algorithm. In *Advances In Neural Information Processing Systems*, pages 2370–2378, 2016.
- [14] James Martens and Ilya Sutskever. Parallelizable sampling of markov random fields. In *Proceedings of the Thirteenth International Conference on Artificial Intelligence and Statistics*, pages 517–524, 2010.
- [15] Radford M Neal. Mcmc using hamiltonian dynamics. *Handbook of Markov Chain Monte Carlo*, 2(11), 2011.
- [16] Aaditya Ramdas, Sashank Jakkam Reddi, Barnabás Póczos, Aarti Singh, and Larry A Wasserman. On the decreasing power of kernel and distance based nonparametric hypothesis tests in high dimensions. In *AAAI*, pages 3571–3577, 2015.
- [17] Bernhard Scholkopf and Alexander J Smola. *Learning with kernels: support vector machines, regularization, optimization, and beyond*. MIT press, 2001.
- [18] EB Sudderth, AT Ihler, WT Freeman, and AS Willsky. Nonparametric belief propagation. In *Computer Vision and Pattern Recognition, 2003. Proceedings. 2003 IEEE Computer Society Conference on*, 2003.
- [19] Martin J Wainwright and Michael I Jordan. Graphical models, exponential families, and variational inference. *Foundations and Trends® in Machine Learning*, 1(1–2):1–305, 2008.